Dual function for Tango1 in secretion of bulky cargo and in ER-Golgi morphology

L. D. Ríos-Barrera[a,1], S. Sigurbjörnsdóttir[a,1,2], M. Baer[b,3], and M. Leptin[a,b,4]

[a]Directors' Research Unit, European Molecular Biology Laboratory, 69117 Heidelberg, Germany; and [b]Institute of Genetics, University of Cologne, 50674 Cologne, Germany

Edited by Kai Simons, Max Planck Institute of Molecular Cell Biology and Genetics, Dresden, Germany, and approved October 16, 2017 (received for review June 27, 2017)

Tango1 enables ER-to-Golgi trafficking of large proteins. We show here that loss of Tango1, in addition to disrupting protein secretion and ER/Golgi morphology, causes ER stress and defects in cell shape. We find that the previously observed dependence of smaller cargos on Tango1 is a secondary effect. If large cargos like Dumpy, which we identify as a Tango1 cargo, are removed from the cell, nonbulky proteins reenter the secretory pathway. Removal of blocking cargo also restores cell morphology and attenuates the ER-stress response. Thus, failures in the secretion of nonbulky proteins, ER stress, and defective cell morphology are secondary consequences of bulky cargo retention. By contrast, ER/Golgi defects in Tango1-depleted cells persist in the absence of bulky cargo, showing that they are due to a secretion-independent function of Tango1. Therefore, maintenance of ER/Golgi architecture and bulky cargo transport are the primary functions for Tango1.

ERES | Sec16 | ERGIC | ER stress | GM130

The endoplasmic reticulum (ER) serves as a major factory for protein and lipid synthesis. Proteins and lipoproteins produced in the ER are packed into COPII-coated vesicles, which bud off at ER exit sites (ERES) and then move toward the Golgi complex where they are sorted to their final destinations. Regular COPII vesicles are 60–90 nm in size, which is sufficient to contain most membrane and secreted molecules. The loading of larger cargo requires specialized machinery that allows the formation of bigger vesicles to accommodate these bulky molecules. Tango1 (Transport and Golgi organization 1), a member of the MIA/cTAGE (melanoma inhibitory activity/cutaneous T cell lymphoma-associated antigen) family, is a key component in the loading of such large molecules into COPII-coated vesicles. Molecules like collagens and ApoB (apolipoprotein B)-containing chylomicrons are 250–450 nm long and rely on Tango1 for their transport out of the ER, by physically interacting with Tango1 or Tango1 mediators at the ERES (1–3).

Tango1 is an ER transmembrane protein that orchestrates the loading of its cargo into vesicles by interacting with it in the ER lumen. The interaction of Tango1 with its cargo then promotes the recruitment of Sec23 and Sec24 coatomers on the cytoplasmic side, while it slows the binding of the outer layer coat proteins Sec13 and Sec31 to the budding vesicle. This delays the budding of the COPII carrier (3). Tango1 also recruits additional membrane material to the ERES from the Golgi intermediate compartment (ERGIC) pool, thereby allowing vesicles to grow larger (4). It also interacts directly with Sec16, which is proposed to enhance cargo secretion (5). A shorter isoform of mammalian Tango1 lacks the cargo recognition domain but nevertheless facilitates the formation of megacarrier vesicles (5, 6).

Apart from bulky proteins, some heterologous, smaller proteins like secreted horseradish peroxidase (ssHRP, 44 kDa) and secreted GFP (27 kDa) also depend on Tango1 for their secretion (7). Unlike for collagen or ApoB, there is no evidence for a direct interaction between Tango1 and ssHRP or secreted GFP. It is not clear why Tango1 would regulate the secretion of these molecules, but it has been proposed that in the absence of Tango1, the accumulation of nonbulky proteins at the ER might be due to abnormally accumulated Tango1 cargo blocking the ER (3, 7); however, this has not been tested experimentally.

Drosophila Tango1 is the only member of the MIA/cTAGE family found in the fruit fly, which simplifies functional studies. Like vertebrate Tango1, the *Drosophila* protein participates in the secretion of collagen (8, 9). And as in vertebrates, ssHRP, secreted GFP, and other nonbulky molecules like Hedgehog-GFP also accumulate in the absence of Tango1 (10, 11). These results have led to the proposal that Tango1 participates in general secretion. However, most of the evidence for these conclusions comes from overexpression and heterologous systems that might not reflect the physiological situation.

Here, we describe a *tango1* mutant allele that we identified in a mutagenesis screen for genes affecting the structure and shape of terminal cells of the *Drosophila* tracheal system (12). Tracheal terminal cells form highly ramified structures with branches of more than 100 μm in length that transport oxygen through subcellular tubes formed by the apical plasma membrane. Their growth relies heavily on membrane and protein trafficking, making them a very suitable model to study subcellular transport. We used terminal cells to study the function of Tango1, and we found that loss of Tango1 affects general protein secretion indirectly, and it also leads to defects in cell morphology and in the

Significance

Exporting bulky molecules poses challenges for cells, since the membrane vesicles that transport normal-sized molecules may not be sufficiently large. The protein Tango1 allows transport vesicles to grow much larger to accommodate bulky cargo. It has been puzzling why many smaller cargos also fail to be transported when Tango1 is absent. We show that this is because bulky cargos "clog up" the transport system, resulting in a general traffic jam. Once the blocking, large cargo is removed, the jam resulting from missing Tango1 is resolved, and other cellular stress signals also subside. However, structural defects in the transport system remain, showing that these are due to a direct requirement for Tango1, independent of its function in transport as such.

Author contributions: L.D.R.-B., S.S., M.B., and M.L. designed research; L.D.R.-B., S.S., and M.B. performed research; L.D.R.-B., S.S., and M.B. analyzed data; and L.D.R.-B., S.S., and M.L. wrote the paper.

The authors declare no conflict of interest.

This article is a PNAS Direct Submission.

[1]L.D.R.-B. and S.S. contributed equally to this work.

[2]Present address: Department of Biochemistry and Molecular Biology, Faculty of Medicine, University of Iceland, 101 Reykjavík, Iceland.

[3]Present address: Institute for Medical Information Processing, Biometry and Epidemiology, Ludwig-Maximilian University of Munich, 81377 Munich, Germany.

[4]To whom correspondence should be addressed. Email: mleptin@uni-koeln.de.

This article contains supporting information online at www.pnas.org/lookup/suppl/doi:10.1073/pnas.1711408114/-/DCSupplemental.

structure of the ER and Golgi. The defects in ER and Golgi organization of cells lacking Tango1 persist even in the absence of Tango1 cargo.

We identify a bulky cargo for Tango1 in *Drosophila*. Our studies have allowed us to explain why, in the absence of Tango1, nonbulky proteins accumulate in the ER despite not being direct Tango1 cargos. We show that these cargos are retained in the ER as a consequence of nonsecreted bulky proteins interfering with their transport. However, the effect of loss of Tango1 on ER/Golgi morphology can be uncoupled from its role in bulky cargo secretion.

Results

Identification of a Mutation in *tango1*. Terminal cells of the tracheal system extend long subcellular branches that transport gas through tubes formed by the apical plasma membrane. The tubes can be easily visualized by bright field microscopy because of the difference in refractive index between the cytoplasm and the gas, providing a simple readout for branch maturation (13). In a screen for genes necessary for tracheal terminal cell branching, we identified a mutation, 2L3443, which caused air-filling defects and reduced branch numbers in homozygous mutant terminal cells (12) (Fig. 1 *A*–*D*). The mutation is embryonic semilethal (33.3% of homozygous embryos failed to hatch), and survivors died at early larval stages. We mapped this mutation by SNP recombination and by complementation tests with deficiencies to the region 26D10-26F3 on the cytogenetic map (*SI Appendix*, Fig. S1*A*). We identified a mutation within the ORF of *tango1* and confirmed it is allelic to other *tango1* mutant alleles (*SI Appendix*, Fig. S1*A′*). The mutation introduces a premature stop codon in amino acid 1341 (arginine to stop codon) downstream of the proline-rich domain (PRD) that results in a truncation of the last 89 amino acids of the predicted protein (*SI Appendix*, Fig. S1 *B* and *C*). The missing segment contains an arginine-rich domain that has no predicted interaction partners. A Tango1-GFP construct expressed under a trachea-specific promoter suppressed the mutant phenotype (Fig. 1 *C* and *D*) and an interfering RNA (*tango1*-IR) expressed specifically in terminal cells caused the same air-filling defects and reduction in branch number (Fig. 2 *A*, *B*, and *E*), confirming that *tango1* disruption was responsible for the branching defects.

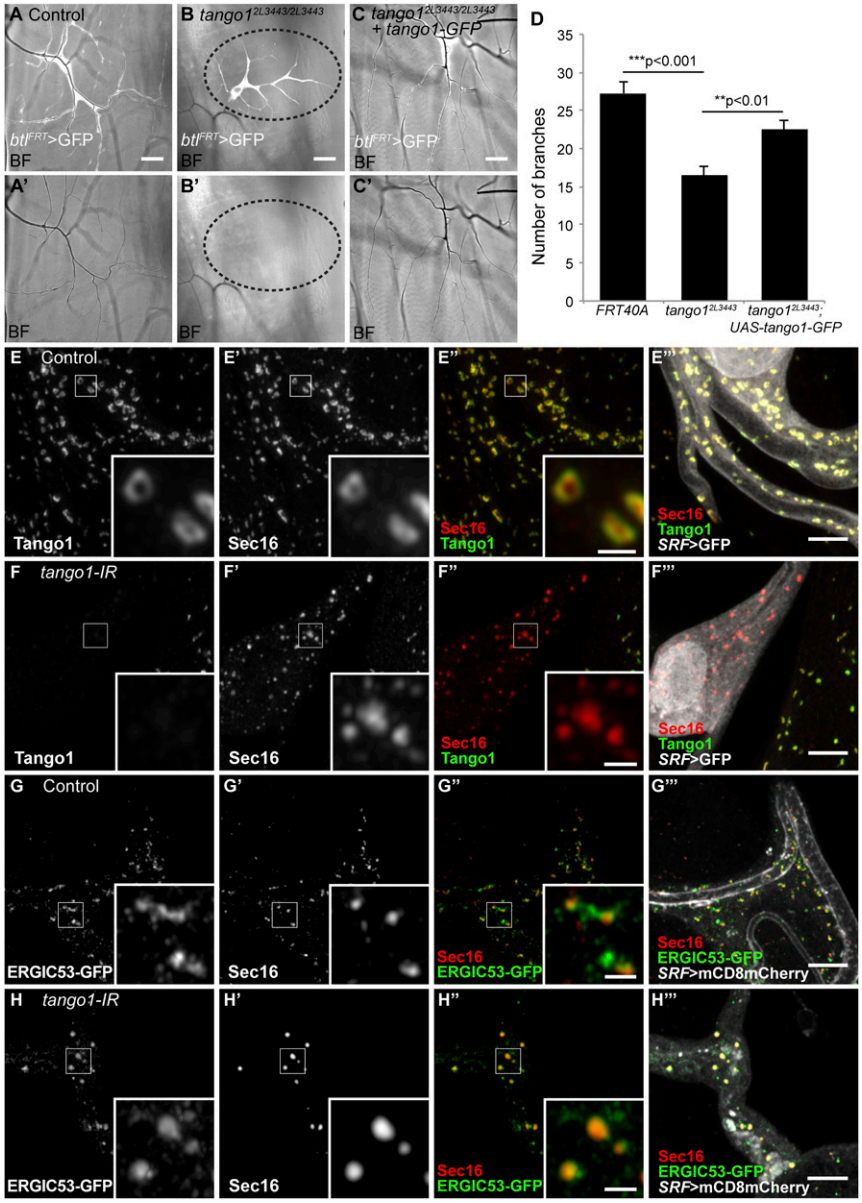

Fig. 1. Effect of loss of Tango1 on cell, ER, and Golgi morphology. (*A*–*C*) Bright field (BF) images of homozygous *tango1*^{2L3443} mutant tracheal cells expressing GFP (*btl*^{FRT} > GFP) allow the visualization of number of branches and the presence of air in terminal cells. Unlike control cells (*A* and *A′*), homozygous *tango1*^{2L3443} cells are not air-filled (area surrounded by dotted line in *B* and *B′*). (*C* and *C′*) Expression of Tango1-GFP in mutant cells suppresses the air-filling defects and reestablishes near-normal number of branches (*D*). Control, $n = 11$; *tango1*^{2L3443}, $n = 14$; *tango1*^{2L3443}+Tango1-GFP, $n = 11$. Bars represent mean ± SEM. Significance was determined using two-tailed *t* test. (*E*–*H*) Airyscan microscopy images of control (*E* and *G*) and *tango1* knockdown cells (*F* and *H*), stained for Tango1 (*E*–*F*) and Sec16 (*E′*–*F′*) and for ERGIC53-GFP (*G*–*H*; fTRG library, expressed at endogenous levels) and Sec16 (*G′*–*H′*). *Insets* in *E*–*H* are magnifications of representative regions, indicated by the white squares. (Scale bars: *A*–*C*, 40 μm; *E*–*H*, 5 μm; *Insets*, 1 μm.)

To determine the role of Tango1 in terminal cells, we first looked at its subcellular distribution. As shown recently for other tissues (10, 14), Tango1 assembles into ring-like structures in tracheal terminal cells and colocalizes with the ERES marker Sec16 (Fig. 1*E*). The truncated Tango1^{2L3443} protein fails to colocalize with Sec16, and Sec16 distribution itself is also altered in *tango1*^{2L3443} mutant cells and upon *tango1* knockdown (Fig. 1*F* and *SI Appendix*, Fig. S2*B*). While in control cells Sec16 particles show a homogenous distribution with a narrow range of sizes with a mean/median of 0.54 μm^2/0.49 μm^2, cells lacking Tango1 contain larger range of sizes with a mean/median of 0.44 μm^2/0.29 μm^2 (Fig. 1 *E* and *F* and *SI Appendix*, Fig. S2 *A* and *B*).

Golgi morphology is also abnormal in cells lacking *tango1* (11). We looked at this at higher resolution with Golgi and ER markers in *tango1*^{2L3443} cells. The distribution of the medial Golgi marker ManII-GFP changes relative to Sec16. In control cells, Sec16 and ManII-GFP are seen as juxtaposed spots, whereas in *tango1*^{2L3443} mutant cells, ManII-GFP seems to enclose Sec16 particles (*SI Appendix*, Fig. S2 *C* and *D*). The cis-Golgi marker GM130 shows a similarly abnormal ring-like appearance, and is also present at significantly higher levels, suggesting an expansion of this compartment (*SI Appendix*, Fig. S2 *E* and *F*). The trans-Golgi marker GalT-GFP (1,4-galactosyltransferase-GFP) and Sec23 form similar rings (*SI Appendix*, Fig. S2 *G–J*), and we therefore assume that Sec23 and Golgi markers become localized to the same doughnut-shaped compartment, consistent with previous studies suggesting the retention of ManII-GFP near the ER (11).

ERGIC53, associated with the retrograde transport pathway, is seen in spots and in extended vesicular structures in normal tracheal cells. The larger structures are often costained for Sec16 at their ends (Fig. 1*G*). RNAi against *tango1* resulted in a more globular structure of the compartment marked by ERGIC53, and its collapse with the Sec16-positive compartment (Fig. 1*H*). This indicates that in the absence of Tango1, ERGIC53 may no longer be able to shuttle back out of the ER into the ERGIC and/or Golgi apparatus. Thus, loss of *tango1* leads to defects both in the ER and in the Golgi apparatus, with the separation between ERGIC53 and Sec16 being lost, and the structure of the Sec23 compartments and the entire Golgi apparatus becoming distorted.

The Role of Tango1 in Terminal Cells: Different Classes of Cargo. Tango1 has been studied for its role in the trafficking of collagen in cultured mammalian cells and in *Drosophila* fat body cells, the main collagen producers in the fly (3, 8). Terminal cells are surrounded by collagen, and although according to expression data collagen may be expressed only at minimal levels in tracheal cells, it was possible that the defects seen in tracheal cells might be due to failures in the secretion of collagen. To test this, we knocked down collagen (encoded by the gene *viking*, *vkg*) specifically in terminal cells. This did not result in any morphological defects of the type that loss of Tango1 caused (*SI Appendix*, Fig. S3*A*). We also compared the effects of knocking down *tango1* either in terminal cells or in the fat body. We found that collagen levels surrounding terminal cells are affected only when *tango1* is knocked down in

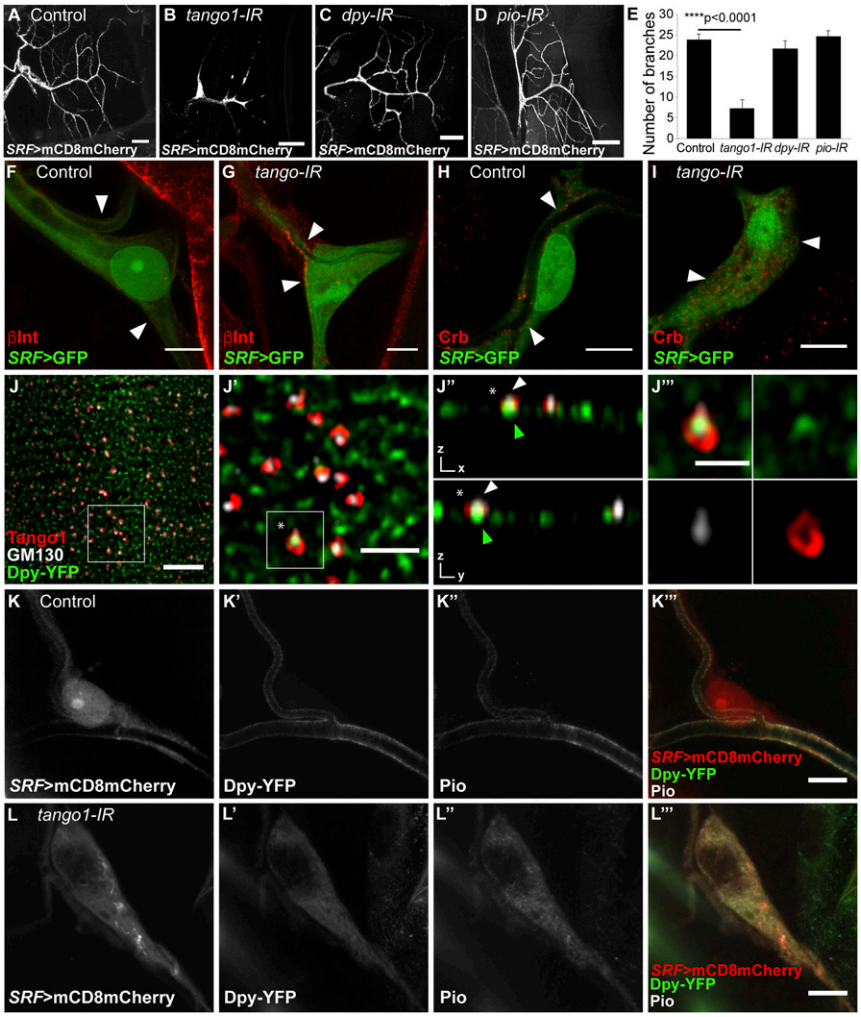

Fig. 2. Function of cargo proteins and their distribution upon loss of Tango1. (*A–E*) Terminal cells were visualized by expressing mCD8mCherry under the terminal-cell–specific driver *SRF-gal4*. (*E*) Manual quantification of branch numbers in terminal cells expressing different RNAi; cells expressing *tango1* RNAi (*B*) have fewer branches than control cells (*A*). Neither *dpy* RNAi (*C*) nor *pio* RNAi (*D*) affect branch numbers. Control, $n = 8$; *tango1-IR*, $n = 9$; *dpy-IR*, $n = 8$; *pio-IR*, $n = 9$. Bars represent mean ± SEM. Significance was determined using two-tailed *t* test. (*F* and *G*) Confocal projections of control (*F*) and *tango1-IR* (*G*) terminal cells expressing *SRF* > GFP and stained for βPS integrin (βInt). Arrowheads point to βInt localization. (*H* and *I*) Confocal projections of control (*H*) and *tango1-IR* (*I*) terminal cells expressing *SRF* > GFP and stained for Crb. Arrowheads point to Crb localization. (*J*) Airyscan images of details of tracheal dorsal trunk cells expressing Dpy-YFP and stained for Tango1 and Golgi marker GM130. White squares indicate the magnified, representative regions in *J′–J‴*. (*J′*) Magnification of the area marked in *J*. (*J″*) Orthogonal views of a single plane from *J′*. The white arrowhead points to GM130 signal and the green arrowhead points to Dpy-YFP signal associated to Tango1. (*J‴*) Magnification of the area marked in *J′*. Asterisks in *J′* and *J″* show the Tango1 ring magnified in *J‴*. (*K* and *L*) Confocal projections of control (*K*) and *tango1-IR* (*L*) terminal cells expressing *SRF* > mCD8mCherry (*K* and *L*) and Dpy-YFP (*K′* and *L′*) and stained for Pio (*K″* and *L″*). [Scale bars: *A–D*, 40 μm; *F–I*, *K*, and *L*, 10 μm; *J*, 5 μm; *J′*, 2 μm (also applies to *J″*); *J‴*, 1 μm.]

the fat body but not when it is absent in terminal cells (*SI Appendix*, Fig. S3 *B–G*). These experiments show first that the collagen surrounding terminal cells is not produced by the terminal cells but mostly, if not entirely, by the fat body, and secondly, that the defects resulting from *tango1* loss of function in terminal cells cannot be explained by a defect in the transport of collagen.

If the defects in *tango1* mutant terminal cells cannot be explained by failure of collagen secretion, then they must be due either to a failure to transport to the cell surface other molecules essential for tracheal function, or to a function unrelated to the secretion of specific substrates (for example, a global failure within the secretory pathway).

We analyzed the distribution of a range of cell surface and secreted proteins in Tango1-depleted terminal cells. These included markers for the basal and apical cell membranes, because morphological defects in epithelial cells are often associated with defective cell polarity. The localization of βPS integrin at the outer, basal membrane of the cell was not affected by *tango1* knockdown (Fig. 2 *F* and *G*). By contrast, the apical membrane protein Crumbs (Crb), normally present at the luminal plasma membrane (Fig. 2*H*), failed to reach its normal destination and was instead found dispersed throughout the cytoplasm (Fig. 2*I*). These observations favor a role for Tango1 in the transport of specific proteins rather than in general secretion.

Since the suggested role for Tango1 is to aid the secretion of very large cargos, we examined the distribution of Dumpy (Dpy), the largest protein encoded in the *Drosophila* genome, with a size of 2.5 MDa and a length of 800 nm (15, 16). Dpy contains EGF-repeat domains and a Zona Pellucida (ZP) domain. It mediates the attachment between cells and the chitinous apical extracellular matrix (aECM), through its interaction with Pio, a ZP transmembrane protein (17). We visualized Dpy through a YFP insertion at the *dpy* locus that results in a fusion protein expressed at endogenous levels, Dpy-YFP (18).

In cells of the tracheal dorsal trunks, we distinguished two pools of Dpy: one that was secreted and was seen within the lumen of the trachea, the other in the cytoplasm, in the form of spots, which were presumably vesicles containing Dpy on its secretion route (Fig. 2*J*). We found that a subset of the Dpy particles was partly or fully surrounded by Tango1 and in close proximity to the Golgi marker GM130 (Fig. 2 *J–J‴*). In terminal cells, Dpy-YFP is present in the lumen of the cells, where it is enriched at the plasma membrane, together with its binding partner Pio (Fig. 2*K*). In *tango1* knockdown terminal cells, neither Dpy-YFP nor Pio were found in the lumen, and they instead accumulated in the cytoplasm (Fig. 2*L*).

To test whether the mislocalization of any of the molecules that we analyzed was responsible for the defects seen in tracheal cells, we depleted Dpy and Pio from terminal cells. Neither *dpy* nor *pio* knockdown produced air-filling defects or a reduction in the number of branches (Fig. 2 *C–E*), despite efficient silencing of *pio* expression (*SI Appendix*, Fig. S6 *A* and *B*). Therefore, the morphological defects resulting from loss of Tango1 cannot be explained by inefficient Dpy or Pio secretion. Similarly, mislocalization of Crb is not sufficient to explain the *tango1* loss-of-function phenotype, since *crb* homozygous mutant terminal cells do not show branching defects that resemble the *tango1* phenotype (19).

In summary, regarding the dependence of different cargos on Tango1, we have found three cases: Dpy represents a cargo that fits the expected characteristic of Tango1 substrates of being very large; Crb is a cargo that depends on Tango1 although it is not large; and finally, βPS integrin is a cargo that does not depend on Tango1. To learn more about the rules and generalities of Tango1-dependent secretory cargos, we examined other tissues.

Effect of Tango1 Loss of Function on Dpy in Wing Discs, Glial Cells, and Tendons. Dpy serves as a scaffold that anchors tissues to the aECM and supports tissue shape changes in many organs, and its function has been most extensively studied in the wing disk (18). Knocking down *tango1* in the wing pouch resulted in intracellular accumulation of Dpy-YFP (*SI Appendix*, Fig. S4 *A* and *B*). Loss of Tango1 was again associated with changes in the distribution of Sec16 and a decrease in Sec23. This was particularly evident when *tango1* was knocked down in a stripe across the disk using *ptc-gal4*. We found that in the absence of Tango1, the number of Sec16 particles per area was reduced and Sec23 fluorescence intensity was reduced (*SI Appendix*, Fig. S4 *C–F*).

Tango1 has previously been shown to be active in larval glial cells and pupal tendons (20, 21), and we found that these cell types are surrounded by Dpy-YFP (*SI Appendix*, Fig. S4 *G* and *J*), consistent with expression reports on other developmental stages (16, 22). Depletion of Tango1 resulted in the intracellular accumulation of Dpy-YFP in both tissues (*SI Appendix*, Fig. S4 *H*, *I*, and *K*). We compared the localization of the intracellular Dpy-YFP spots in glial and tendon cells with that of KDEL-RFP, an ER marker. Dpy-YFP colocalized with KDEL-RFP in cells lacking Tango1 (and indeed the entire ER seemed to be filled with Dpy-YFP), suggesting Dpy remains within the ER in these cells (*SI Appendix*, Fig. S4 *I* and *K*). These experiments indicate that the role of Tango1 in Dpy secretion is general, and not restricted to tracheal cells. Whereas the tissues studied so far each have their own, specific cargos that depend on Tango1, they also share Dpy as a common cargo.

Direct and Indirect Effects of Loss of Tango1 on Cargo Accumulation in the Fat Body. Tango1-dependent trafficking has been most thoroughly characterized in the fat body. A number of cargos including collagen are not delivered to the cell surface in fat body cells lacking Tango1, and the structure of the ER and Golgi are abnormal (8, 10). Fat body cells do not express Dpy, and as in tracheal cells, endogenous βPS integrin distribution is not affected by lack of Tango1, although Sec16 also forms aberrant aggregates (*SI Appendix*, Fig. S5 *A* and *B*).

We noticed that independent of size, secretion of several overexpressed molecules was impaired upon *tango1* knockdown in fat body cells. This included Gasp-GFP, with a molecular mass of only 55 kDa (*SI Appendix*, Fig. S6 *C* and *D*), and overexpressed βPS integrin-Venus, although endogenous βPS integrin was unaffected (*SI Appendix*, Fig. S5 *C* and *D*). Previous reports have also shown that in *Drosophila*, the absence of Tango1 leads to the accumulation of other overexpressed small cargos like secreted HRP and GFP, and of Hedgehog-GFP (10, 11). This was also observed in cultured mammalian cells for secreted HRP and GFP (3, 7). In the case of mammalian cells, it was suggested that HRP accumulation was caused by unsecreted collagen blocking the secretory pathway (7). To test whether such a mechanism may explain the failure of smaller molecules to be secreted in *tango1*-deficient fat body cells, we studied whether the reduction of *vkg* would improve the secretion of small cargos by simultaneously knocking down *vkg* and *tango1*. We found that if in addition to *tango1*, we knocked down *vkg*, this resulted in the rescue of the secretion of overexpressed βPS integrin (*SI Appendix*, Fig. S5 *E* and *F*) as well as overexpressed Crb fused to GFP (Crb-GFP, *SI Appendix*, Fig. S7 *A–D*). To exclude an artifactual amelioration of the *tango1*-knockdown phenotype because the second RNAi construct might reduce the efficiency of *tango1* knockdown, in this and further experiments, we compared Tango1 and collagen levels in the double knockdown condition with individual *tango1* and *vkg* knockdowns and found that both targets were equally well silenced in the two conditions (*SI Appendix*, Fig. S7 *E–H*). These results show that both overexpressed βPS integrin-Venus and Crb-GFP can be delivered to the membrane in the absence of Tango1 if collagen is also removed, suggesting that their accumulation upon *tango1* knockdown is an indirect effect of collagen accumulation.

We also wanted to test whether SPARC and laminins, two other cargos known to depend on Tango1 for their secretion (20,

21) (*SI Appendix*, Figs. S6 *E* and *F* and S8 *A*, *B*, *E*, and *F*), might be blocked by collagen accumulation in the fat body. These experiments were inconclusive because loss of collagen itself leads to laminins and SPARC retention in the ER (*SI Appendix*, Figs. S6*G* and S8 *C* and *G*), and simultaneous collagen and Tango1 knockdown therefore did not rescue laminin or SPARC secretion (*SI Appendix*, Figs. S6*H* and S8 *D* and *H*).

Direct and Indirect Effects of Loss of Tango1 on Cargo Accumulation in Glial Cells and in Terminal Cells. Like overexpressed βPS integrin and Crb in the fat body, some of the Tango1-dependent cargos identified in tracheal, glial, wing epithelial, and tendon cells are also not particularly bulky. We therefore investigated whether they might also not be direct substrates of Tango1. These tissues do not express detectable levels of collagen (8, 20, 21), and it was therefore unlikely that unsecreted collagen was the blocking cargo. We therefore wondered whether Dpy, as another large Tango1 cargo might be blocking the secretory pathway.

Glial cells of the larval brain and of the peripheral nervous system have also been shown to need Tango1 for the secretion of laminin chains LanB1 and LanB2 (20). Laminins are assembled into trimers composed of the LanB1, LanB2, and LanA subunits. All subunits are required for trimer secretion, but LanA can also be secreted as a monomer. We found that as has been shown for LanB1 (*SI Appendix*, Fig. S6 *I* and *J*), *tango1* knockdown also resulted in LanA accumulation in the ER (*SI Appendix*, Fig. S9 *A*, *B*, and *E*). It was puzzling that LanA was retained at the ER in glial cells lacking Tango1, considering that it should be able to be secreted as a monomer even when LanB1 and LanB2 are not secreted (23). To test if accumulated intracellular Dpy might be responsible for this, we knocked down *tango1* and *dpy* simultaneously. We found that the defective secretion of both LanA and LanB1 caused by lack of Tango1 was rescued by also silencing *dpy* (*SI Appendix*, Figs. S6*L* and S9 *D* and *E*; controls for knockdown efficiency in *SI Appendix*, Fig. S10 *A*–*D*).

In tracheal cells, where Crb delivery to the membrane was completely abolished by *tango1* knockdown (Figs. 2 *H* and *I* and 3 *A* and *B*), the additional knockdown of *dpy* caused Crb membrane localization to be reestablished (Fig. 3*D*; controls for knockdown efficiency in *SI Appendix*, Fig. S10 *E*–*H*). In summary, the effect of loss of Tango1 on a broad range of cargos is indirect, with the proximal effect being the retention of one or perhaps a small number of direct substrates, which in turn blocks the proper trafficking of other molecules.

ER Stress and Cell Morphology. Our results so far pointed toward *tango1* loss of function in terminal cells and in other tissues affecting not only the secretion of its own cargo, but also that of

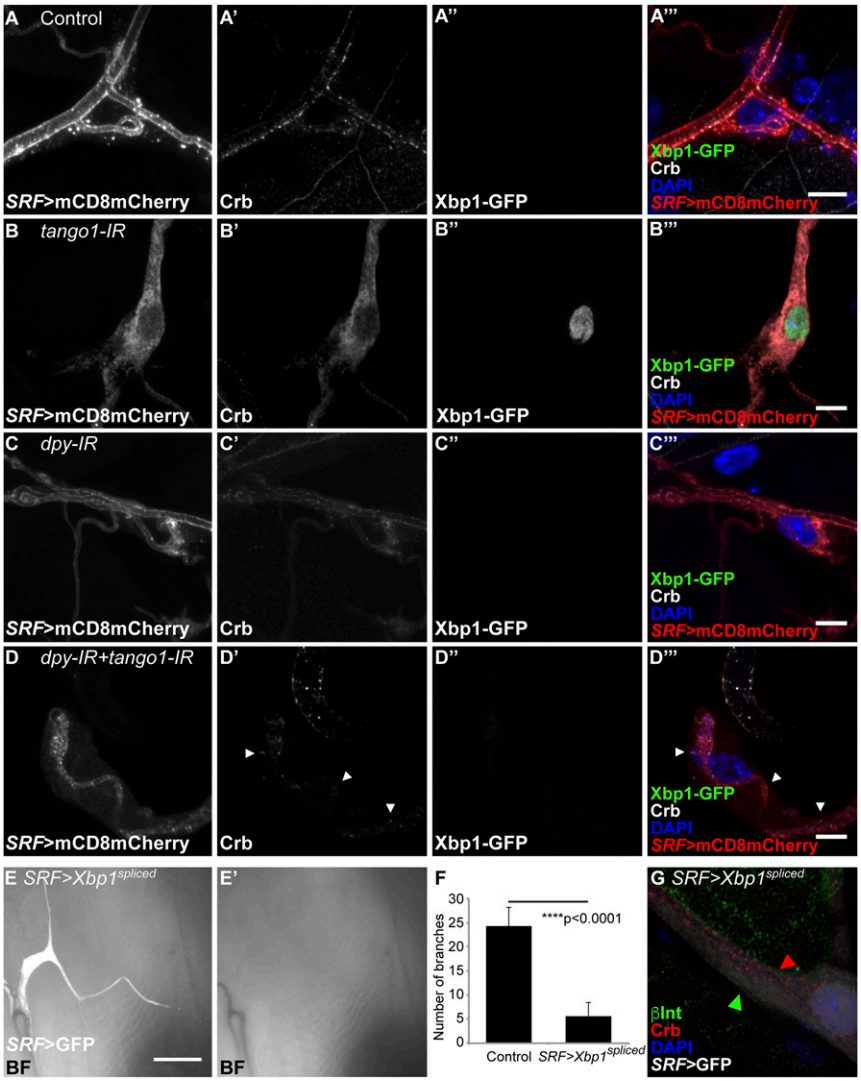

Fig. 3. Effect of *tango1* and *dpy* knockdown on Crb and the ER stress response. (*A*–*D*) Terminal cells expressing mCD8mCherry (*A*–*D*) and Xbp1-GFP (*A*″–*D*″) under *SRF-gal4*. Xbp-1-GFP is translated and accumulated in the nucleus only after activation of the ER-stress response. (*A*′–*D*′) In control (*A*′ and *A*″) and *dpy-IR* cells (*C*′ and *C*″), Crb localizes to the luminal membrane and Xbp1-GFP is not detectable. In *tango1-IR* cells (*B*′ and *B*″), Crb does not reach the membrane and Xbp1-GFP accumulates in the nucleus. These defects can be suppressed by additionally knocking down *dpy* (*D*′ and *D*″). (*E*–*G*) Terminal cells expressing GFP and the ER stress response target Xbp1 under *SRF-gal4*. (*E* and *E*′) Bright field (BF) imaging shows lack of air in the tracheal branches. (*F*) Quantification of number of branches in tracheal cells expressing Xbp1 under *SRF-gal4*. Bars represent mean ± SD. Control, $n = 5$, *SRF* > *Xbp1*^{spliced}, $n = 8$. Significance was assessed using Student's *t* test. (*G*) Terminal cells expressing *Xbp1*^{spliced} where stained against βInt and Crb. Arrowheads point to the normal distribution of both proteins. (Scale bars: *A*–*D* and *G*, 10 μm; *E*, 40 μm.)

others as a side effect of the ER being blocked by unsecreted cargo. A documented consequence of protein retention at the ER is the activation of the ER stress response (20). We therefore investigated whether the ER stress response was activated upon loss of Tango1. To test this, we used the marker Xbp1-GFP, which is posttranscriptionally up-regulated in response to ER stress (24, 25). We observed high levels of Xbp1-GFP in terminal cells lacking Tango1, but not in control or *dpy-IR* cells (Fig. 3 *A*–*C*).

When *tango1* and *dpy* were simultaneously depleted, Xbp1-GFP was no longer up-regulated (see Fig. 7*D*). These results suggested that the activation of the ER stress response is not a direct consequence of loss of Tango1, but instead, the result of abnormal protein accumulation in the ER.

The original phenotype for which we identified the *tango1* mutation was defective terminal cell morphology. We argued above that this was not due to the loss of Dpy or Pio at the cell surface (Fig. 2 *C*–*E*). Having found that ER stress and indirect retention of small cargos could be suppressed by removing primary cargos, we wondered whether the morphological defects were also secondary to protein accumulation, or if they revealed a direct function of Tango1 independent of its role in secretion of Dpy. We found that the defects in branch number and branch air filling seen in *tango1* knockdown cells were significantly suppressed if *dpy* was also silenced (Fig. 4). This suggests that most of the deleterious effect of Tango1 depletion on terminal cell morphology is a consequence of abnormal Dpy accumulation. Since loss of *dpy* itself has no effect on cell morphology, Dpy and the resulting failure in protein secretion or ER stress may be the cause for the defects in cell shape.

ER stress triggers the splicing of *Xbp1* mRNA by Ire1, allowing the synthesis of the Xbp1 transcription factor. Experimental expression of a spliced *Xbp1* mRNA ($Xbp1^{spliced}$) constitutively activates this branch of the ER stress response. Expression of $Xbp1^{spliced}$ in terminal cells led to reduced branching and to air-filling defects similar to the defects caused by the loss of *tango1* (Fig. 3 *E* and *F*). However, the distribution of βPS integrin and Crb remained unaffected in these cells (Fig. 3*G*). These results show that while the activation of the ER-stress response is not responsible for Crb mislocalization, it may be partly responsible for the morphological defects we observe in cells lacking *tango1*. Therefore, the effect that loss of Tango1 and accumulation of Dpy have on cell shape is likely indirect and caused by the ER-stress response. By contrast, the accumulation of other cargos is not caused the stress response.

Possible Mechanisms for Cargo Retention. Dpy could be affecting the secretion of other proteins in a number of different ways. For example, it could compromise the capacity of the ER to support proper folding and processing of proteins, leading to protein retention in association with chaperones, or Dpy might be competing with other molecules for ERES availability.

If the cargos for which we observe defects in transport were retained because of incomplete folding, we would expect them to be associated with chaperones. We find that Calnexin, an ER chaperone involved in folding quality control (26), is up-regulated in wing disk cells after *tango1* knockdown (*SI Appendix*, Fig. S4*E*). We therefore tested whether the cargos we have been studying in tracheal cells were associated with Calnexin. In terminal cells lacking Tango1, Calnexin is strongly enriched at the sites of intracellular accumulation of Dpy (*SI Appendix*, Fig. S11 *B* and *H*). In contrast, other retained molecules like Pio and Crb are seen preferentially in areas of low Calnexin concentration (*SI Appendix*, Fig. S11 *D*, *F*, and *G*). From these results, we conclude that loss of Tango1 does not lead to a general defect in protein folding, and that lack of proper folding therefore does not account for the inability of Pio and Crb to enter the secretory pathway.

We then looked whether accumulated cargos would reach the ERES at all. We found that in cells lacking Tango1, both Dpy

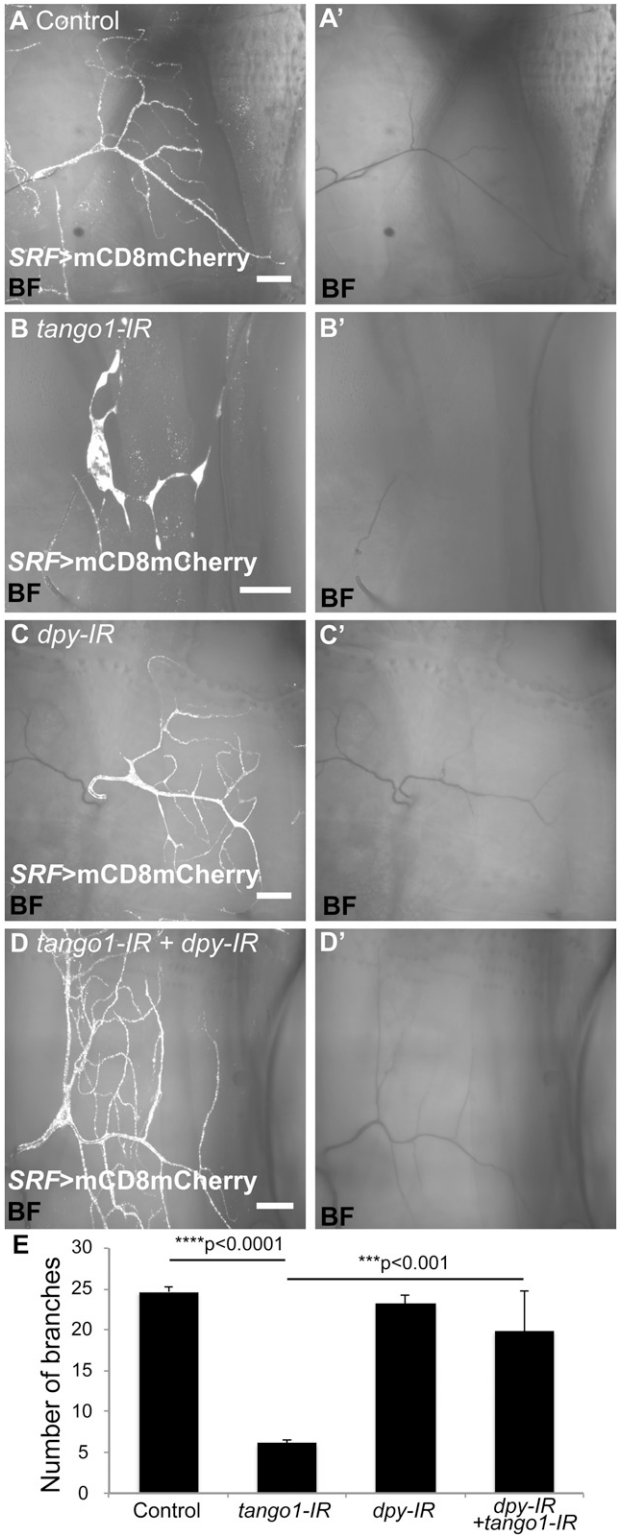

Fig. 4. Rescue of cell morphology in *tango1*-depleted cells by removal of Dpy. (*A*–*D*) Bright field (BF) and mCD8mCherry expression under the terminal cell-specific driver *SRF-gal4*. In control (*A* and *A*′) and *dpy-IR* cells (*C* and *C*′), branches are filled with gas, whereas the absence of *tango1* leads to failure of air-filling and reduced branching (*B* and *B*′). Both defects are suppressed by additionally knocking down *dpy* (*D* and *D*′). (*E*) Quantification of branching in *A*–*D*. Bars represent mean ± SEM. Control, $n = 4$; *tango1-IR*, $n = 9$; *dpy-IR*, $n = 8$; *tango1-IR+dpy-IR*, $n = 8$. Significance was determined using one-way ANOVA and Tukey's multiple comparisons test.

and Crb are at least partially seen in association with Sec16 particles (Fig. 5 *B* and *D*). Consistent with this, we also observed Dpy and Crb in the proximity of Sec23 aggregates (*SI Appendix*, Fig. S12 *B* and *D*). This means that both primary and secondary cargos can reach the ERES, and to some extent COPII vesicles, although they are ultimately not successfully trafficked out of the ERES.

Separable Roles for Tango1 on ER/Golgi Architecture and Secretion. Since failure to secrete a range of proteins and defective cell morphology were indirect effects of the loss of Tango1, we wondered whether this might also be true for the distorted Golgi and ER, and whether these might also be caused by the abnormal accumulation of large cargo (in this case Dpy). We found that when Dpy was removed, the colocalization of ERGIC53 with Sec16 we saw in cells lacking Tango1 was reduced, but not completely reversed (*SI Appendix*, Fig. S13 *D* and *E*). Thus, ERGIC53 is retained at the ERES in the absence of Tango1, and aberrant accumulation of Dpy in the ER and at the ERES exacerbates this condition.

The distorted structure of the ERES in cells lacking Tango1, as seen by Sec16 organization, was not restored when Dpy was removed, and we still observed a wide range of Sec16 particle sizes and staining intensities (Fig. 6 *D*–*F*). Similarly, large Sec23 ring-like aggregates surrounding the ERES were also not suppressed by knocking down *dpy* in Tango1-depleted cells (*SI Appendix*, Fig. S14 *D* and *E*). Similar results were obtained for GM130, a Golgi marker; while control and *dpy-IR* cells showed a homogeneous size distribution of GM130-stained particles (Fig. 7 *A* and *C*), in *tango1* and double knockdown cells, the distribution of GM130 is

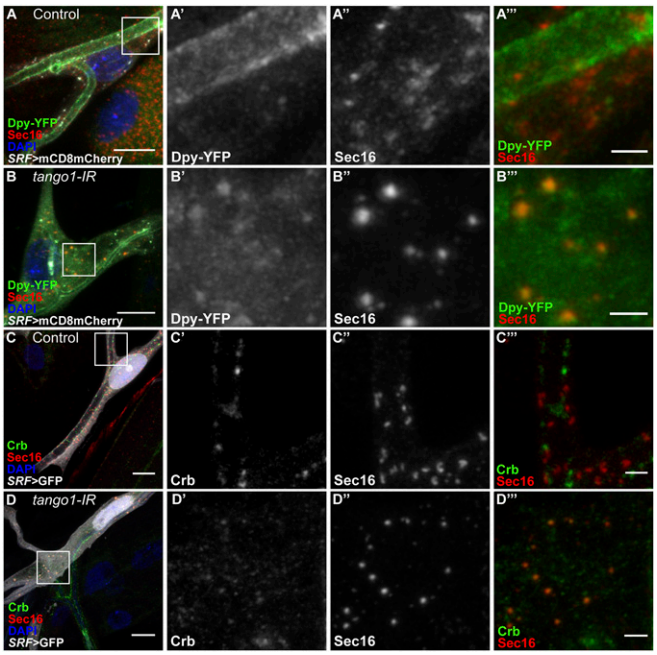

Fig. 5. Distribution of cargo proteins and Sec16 in cells lacking Tango1. White boxes in *A*–*D* are representative fields magnified in *A′*–*A‴*, *B′*–*B″*, *C′*–*C‴*, and *D′*–*D‴*, respectively. (*A* and *B*) Confocal projections of terminal cells expressing mCD8mCherry under *SRF-gal4*, endogenously tagged Dpy-YFP (*A′* and *B′*) and stained for Sec16 (*A″* and *B″*). While in control cells Dpy-YFP is seen at the luminal membrane (*A*–*A‴*), in cells lacking *tango1* Dpy-YFP shows a cytoplasmic distribution that partially overlaps with Sec16 (*B*–*B‴*). (*C* and *D*) Confocal projections of terminal cells expressing GFP under *SRF-gal4* and stained for Sec16 and Crb. While in control cells Crb localizes to the luminal membrane (*C*–*C‴*), in cells lacking *tango1* Crb shows a cytoplasmic distribution that partially overlaps with Sec16 (*D*–*D‴*). (Scale bars: *A*–*D*, 10 μm; *A‴*–*D‴*, 2 μm.)

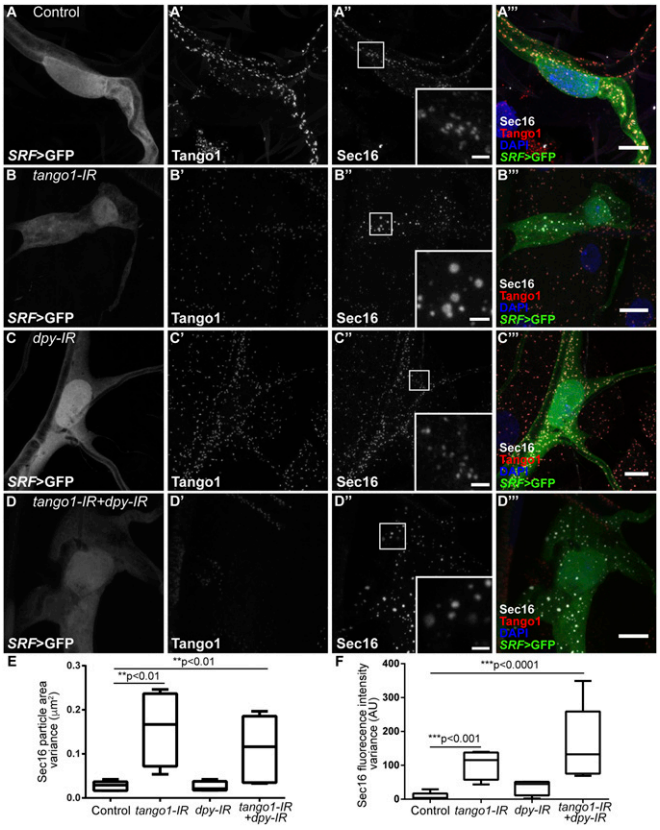

Fig. 6. Effect of loss of Tango1 and Dpy on Sec16 distribution. (*A*–*D*) Tango1 (*A′*–*D′*) and Sec16 (*A″*–*D″*) in terminal cells expressing GFP under *SRF-gal4*. In control (*A*–*A‴*) and *dpy-IR* cells (*C*–*C‴*), Sec16 particles are homogeneous in size and fluorescence intensity; in *tango1-IR* cells, Sec16 particle size and fluorescence intensity is variable (*B*–*B‴*), and this variability is not altered by simultaneously removing Dpy (*D*–*D‴*). Insets in (*A″*–*D″*) are magnifications of representative regions, indicated by the white squares. (*E* and *F*) Variance of Sec16 particle size (*E*) and Sec16 fluorescence intensities (*F*). Control, $n = 5$; *tango1-IR*, $n = 4$; *dpy-IR*, $n = 4$; *tango1-IR*+*dpy-IR*, $n = 5$. Significance was determined using one-way ANOVA and Sidak's multiple comparisons test. (Scale bars: 10 μm; *Insets*, 2 μm.)

altered and it also appears in ring-like structures (Fig. 7 *B* and *D*). Given that in the double knockdown cells Dpy is no longer retained in the ER and that secretion of other molecules is reestablished, these results indicate that Tango1 has an additional function in maintaining ER-Golgi morphology that is independent of its role in bulky cargo transport.

Discussion

We have described a role of Tango1, which we initially identified through its function in tracheal terminal cells and other tissues in *Drosophila* embryos, larvae, and pupae. Due to their complex shapes and great size, terminal cells are a well-suited system to study polarized membrane and protein trafficking, with the easily scorable changes in branch number and maturation status providing a useful quantitative readout that serves as a proxy for functional membrane and protein trafficking machinery. Moreover, our analyses are conducted in the physiological context of different tissues in the intact organism.

Nature of the *tango1*^{2L3443} Allele. The loss-of-function allele *tango1*^{2L3443} has a stop codon eight amino acids downstream of the PRD domain and eliminates the 89 C-terminal amino acids of the full-length protein. It is unlikely that the mutation leads to a complete loss of function. First, terminal cells expressing an RNAi

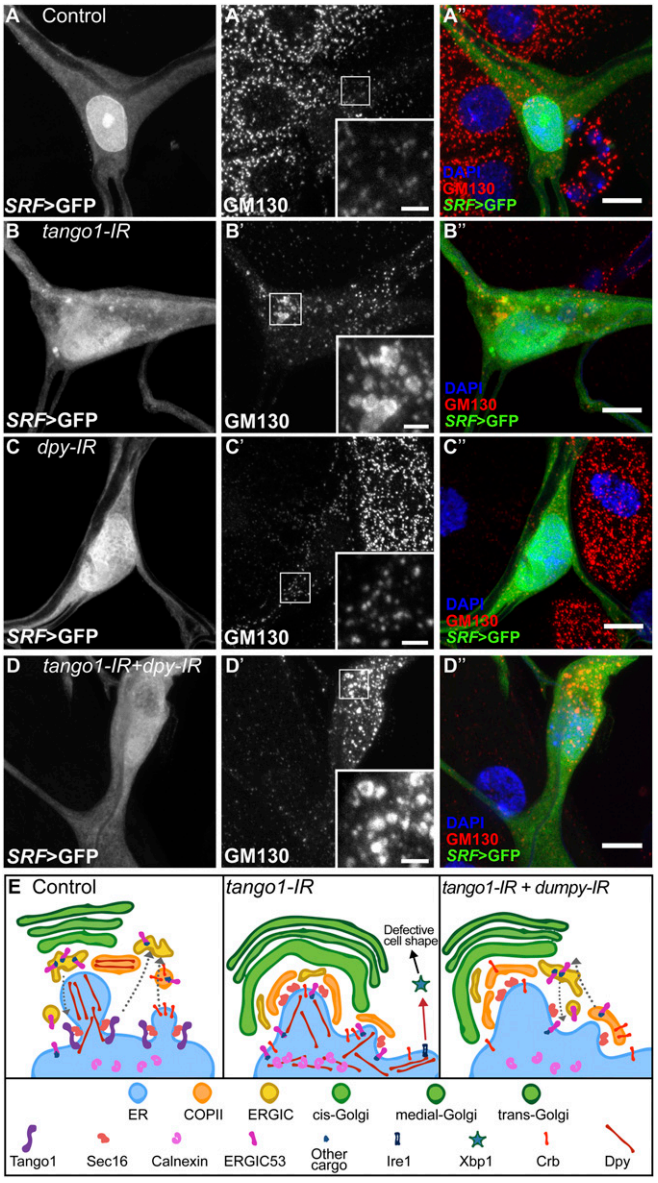

Fig. 7. Effect of loss of Tango1 and Dpy on GM130 distribution. (*A–D*) Terminal cells expressing GFP under *SRF-gal4*, and stained for the Golgi marker GM130 (*A′–D′*). In control (*A–A″*) and *dpy-IR* cells (*C–C″*), the distribution and size of GM130-labeled structures is homogeneous, whereas in *tango1-IR* cells, GM130 is seen in heterogeneous aggregates (*B–B″*). Knocking down *dpy* in *tango1*-IR cells does not rescue GM130 distribution (*D–D″*). *Insets* in *A′–D′* are magnifications of representative regions, indicated by the white squares. (Scale bars: 10 μm; *Insets*, 2 μm.) (*E*) Model showing the role of Tango1 in Dpy trafficking and the indirect consequences of Dpy blockage. In the absence of Tango1, the structure of the ER, COPII, and Golgi apparatus are changed, ERGIC53 is retained in the ER, and the ER-stress response is activated. Additionally, neither Dpy nor Crb reach the plasma membrane. If Dpy levels are reduced, ERGIC53 shuttles out of the ER, the ER-stress response is no longer active and Crb can be secreted. However, the ER, COPII, and Golgi morphology are not restored.

construct against *tango1* show stronger defects, with fewer branches per cell than homozygous *tango1*^{2L3443} cells. Second, the mutant protein appears not to be destabilized nor degraded, but instead is present at apparently normal levels, albeit at inappropriate sites. Predictions of the deleted fragment of the protein suggest it is disorganized and that it contains an arginine-rich domain that has no known interaction partners and that is not present in human Tango1. In homozygous mutant terminal cells, the mutant Tango1^{2L3443} protein fails to localize at ERES. In mammalian Tango1, the Sec16-interacting region within the PRD domain is necessary for the localization of Tango1 to the ERES and for its interaction with Sec23 and Sec16 (3, 5), but since this domain is fully present in Tango1^{2L3443}, our results mean that either the missing 89 C-terminal amino acids contain additional essential localization signals, or that the PRD domain is structurally affected by the truncation of the protein. We consider the latter less likely, as a truncation eight amino acids downstream of the PRD domain is unlikely to destabilize the polyproline motifs, especially as the overall stability of the protein does not seem to be affected. Furthermore, this region shows a high density of phosphoserines (Ser-1345, Ser-1348, Ser-1390, and Ser-1392; ref. 27), suggesting it might serve as a docking site for adapter proteins or other interactors.

Possible Causes of the Cellular Morphological Defects. Terminal cells lacking Tango1 have fewer branches than control cells and are often not properly filled with air. This loss-of-function phenotype is not due to a direct requirement for Tango1, as it is suppressed by the simultaneous removal of Dpy. It also cannot be explained by the individual loss of *crb*, *pio*, or *dpy*, since knocking down any of these genes has no effect on cell morphology. Instead, we propose that the cell morphological defect is due at least in part to the activation of the ER stress response, since expression of Xbp1 is sufficient to recapitulate the phenotype. Xbp1 regulates the expression of genes involved in protein folding, glycosylation, trafficking, and lipid metabolism (28). It is possible that one or a small number of specific genes downstream of Xbp1 are responsible for defective branch formation or stability, but the phenotype could also be a secondary consequence of the physiological effects of the ER stress response itself, for example, a failure to deliver sufficient lipids and membrane from the ER to the apical plasma membrane.

Dumpy, a Cargo of Tango1. Collagen, with a length of 300 nm, and ApoB chylomicrons with a diameter of >250 nm, have both been biochemically validated as Tango1 cargos (1, 3). These molecules are not expressed in terminal cells (this work and ref. 29), and therefore it was clear that Tango1 must have a different substrate in these cells. Given that Tango1 is known for the transport of bulky cargo, that Dpy is the largest *Drosophila* protein at 800 nm length, and that Dpy vesicles are associated with Tango1 rings in tracheal cells, we propose that Dpy is a further direct target of Tango1. Colocalization of Tango1 with its cargo has also been observed in other tissues: with collagen in *Drosophila* follicle cells and with ApoB in mammalian cell lines (1, 9).

No regions of sequence similarity that could represent Tango1-binding sites have been found in Tango1 cargos. There are several possible explanations for this. First, these proteins may contain binding motifs, but the motifs are purely conformational and not represented in a linear amino acid sequence. There is no evidence for or against this hypothesis, but it would be highly unusual, and there is support for alternative explanations. Thus, as a second possibility, all three proteins may require Tango1 for their secretion, but variable adapters could mediate the interactions. In vertebrates, Tango1 can indeed interact with its cargo through other molecules; for instance, its interaction with collagen is mediated by Hsp47 (30). However, in *Drosophila*, there is no Hsp47 homolog (31). In the case of ApoB, it has been suggested that microsomal triglyceride transfer protein (MTP) and its binding partner, protein disulphide isomerase (PDI), might associate with Tango1 and TALI to promote ApoB chylomicrons loading into COPII vesicles. Evidence supporting this is that the lack of MTP leads to ApoB accumulation at the ER (1, 2). It is not known if secretion of other Tango1 cargos like collagen or Dpy also depends on MTP and PDI, but PDI is known also to form a complex with the collagen-modifying enzyme prolyl 4-hydroxylase

(32). We have previously shown that terminal cells lacking MTP show air-filling defects and fail to secrete Pio and Uninflatable to the apical membrane, and that loss of MTP in fat body cells also affects lipoprotein secretion (29), as it does in vertebrates. Since cells lacking MTP or Tango1 have similar phenotypes, it is plausible that the MTP function might be connected to the activity of Tango1.

Clogging of the ER. We interpret our data to mean that in the absence of Tango1, primary cargo accumulates in the ER, and in addition, there are secondary, indirect effects that can be suppressed by reducing the Tango1 cargo that overloads the ER. The secondary effects include activation of the ER stress response and intracellular accumulation of other trafficked proteins like Crb, laminins, and overexpressed proteins and probably also the accumulation of heterologous proteins like secreted HRP or GFP in other systems (7).

Our data suggest that primary and secondary cargo reach the ERES but fail to be trafficked further along the secretory pathway. In this model, primary cargo, probably recruited by adaptors, would be competing with other secondary cargo for ERES/COPII availability, creating a bottleneck at the ERES. This is consistent with recent experiments that show that in *tango1*-knockdown HeLa cells, VSVG-GFP trafficking does not stop completely, but is delayed. Furthermore, in these experiments, VSVG-GFP is mostly seen in association with Sec16 and Sec31 (5), supporting the clogging model.

Different Sensitivities of βPS Integrin and Crb to Loss of Tango1. It is not immediately clear why cargo accumulation in terminal cells lacking Tango1 affects the secretion of Crb but not of βPS integrin. While we look at steady states in our analyses, Maeda et al. (5) have measured the dynamics of secretion and find that loss of Tango1 leads to a reduced rate of secretion of VSVG-GFP, an effect that we would have missed for any proteins we classify as not affected by loss of Tango1. Irrespective, we can think of a range of mechanisms that might be responsible for this difference, including alternative secretion pathways and differences in protein recycling. Alternative independent secretory pathways have been reported in different contexts. For instance, while both αPS1 and βPS integrin chains depend on Sec16 for their transport, the αPS1 chain can bypass the Golgi apparatus and can instead use the dGRASP-dependent pathway for its transport (33). It would be possible then that in terminal cells, βPS integrin is also trafficked through an alternative pathway that is not affected by loss of Tango1. Similarly, tracheal cells lacking Sec24-CD accumulate Gasp, Vermiform, and Fasciclin III, but not Crb (34), supporting a role for alternative secretion pathways for different proteins, as already proposed by Nogueira et al. (7). Following this logic, overexpressed βPS integrin would then also be trafficked through a different route from that of the endogenous βPS integrin, possibly because of higher expression levels or because of the presence of the Venus fused to the normal protein.

Other Secondary Tango1 Cargos in Fat Body: Interdependence of Extracellular Matrix Proteins. *Drosophila* Tango1 was initially found to facilitate collagen secretion in the fat body. More recently, the accumulation of other nonbulky proteins at the ER in the absence of Tango1 has led to the proposal of two models to explain these results: one in which Tango1 regulates general secretion (10), and the second one where Tango1 is specialized on the secretion of ECM components (10, 21), since loss of Tango1 leads to the accumulation of the ECM molecules SPARC and collagen (21). Our results suggest a third explanation, where cargo accumulation in the ER might not necessarily be a direct consequence of only the loss of Tango1. Instead, in addition to depending on Tango1, some proteins of the ECM appear also to depend on each other for their efficient secretion. This is the case for laminins LanB1 and LanB2, which require trimerization before exiting the ER, while LanA can be secreted as a monomer (23). Loss of collagen itself leads to the intracellular accumulation of ECM components in fat body cells, such as the laminins and SPARC. Conversely, SPARC is required for proper collagen and laminin secretion and assembly in the ECM (8, 31, 35). Furthermore, intricate biochemical interactions take place between ECM components (36). Hence, due to the complex genetic and biochemical interactions between ECM components, the dependence of any one of them on Tango1 is difficult to determine without further biochemical evidence. The concept of interdependent protein transport from the ER as such is not new, as it has also been observed in other systems, for instance in immune complexes. During the assembly of T-cell receptor complexes and IgM antibodies, subunits that are not assembled are retained in the ER and degraded (37).

Nevertheless, our observations in glial cells, which express laminins but not collagen, allow us to at least partly separate these requirements. We find that laminins are accumulated due to general ER clogging and not because they rely on Tango1 for their export. This is based on our observations that once the protein causing the ER block is removed, laminin secretion can continue in the absence of Tango1. It is still unclear why glial cells can secrete laminins in the absence of collagen whereas fat body cells cannot, but presumably laminin secretion can be mediated by different, unidentified cargo receptors expressed in glial cells.

A Direct Role for Tango1 in ER-Golgi Organization. We found that Sec16 forms aberrant aggregates in cells lacking Tango1, as in mammalian cell lines (3), and that the number of Sec16 particles is reduced. Other studies have shown that Tango1 overexpression produces larger ERES (10), and that Tango1 and Sec16 depend on each other for localization to ERES (5). In addition, as shown here and by others, lack of Tango1 also affects the distribution of Golgi markers (4, 10, 11). Thus, Tango1 influences not only the trafficking of cargos, but also the morphology of the secretory system.

It had been suggested that the disorganization of ER and Golgi apparatus in cells lacking Tango1 might be an indirect consequence of the accumulation of Tango1 cargo (3). The work of Maeda et al. has provided a possible explanation for the molecular basis, and proposed that Tango1 makes general secretion more efficient, but it has not formally excluded the possibility that the primary cause for the observed defects is secretory protein overload. We have now shown that this is not the case: In the absence of Tango1, we still observe an aberrant ER and Golgi morphology even after we have removed the main primary substrates of Tango1 and, thereby, restored secretion of other molecules and prevented the ER stress response.

ERGIC53 accumulates at the ERES in the absence of Tango1, and this can be partly reversed by removing *dpy*. This is in apparent contradiction to findings in mammalian cells where Tango1 was necessary for the recruitment of membranes containing ERGIC53 to the budding collagen megacarrier vesicle (4, 7). However, ERGIC53 also has Tango1-independent means of reaching the ER (4, 7). Our results indicate that its retrieval from the ER to the ERGIC compartment depends directly or indirectly partly on Tango1. As a cargo receptor for glycoproteins (38), ERGIC53 may be retained at the ERES as a consequence of the accumulation of its own cargo at these sites. This would mean that it cannot be delivered back to the ERGIC or the cis-Golgi apparatus for further rounds of retrograde transport, which may, in turn, be an explanation for the enlargement of the GM130 compartment we see after Tango1 knockdown.

The finding that Tango1-depleted cells have a functional secretory pathway despite the ER-Golgi disorganization was unexpected. Stress stimuli like amino acid starvation (but not ER stress response itself) lead to Sec16 translocation into Sec bodies and inhibition of protein secretion (39). However, uncoupling of ER-Golgi organization from functional secretion has also been

observed in other contexts. Loss of Sec23 or Sec24-CD leads to KDEL appearing in aggregates of varying sizes and intensities similar to those we observe for Sec16 and for KDEL-RFP in cells lacking *tango1* (34). Also, GM130 is reduced in Sec23 mutant embryos. Despite these structural problems, these embryos do not show generalized secretion defects and also do not affect the functionality of the Golgi apparatus, as determined by glycosylation status of membrane proteins (34).

Thus, Tango1 appears to have an important structural function in coordinating the organization of the ER and the Golgi apparatus, and this, in turn, may enhance vesicle trafficking. This fits with the role of Tango1 in recruiting ERGIC membranes to the ERES (4), and also with the effects of loss of Tango1 in the distribution of ER and Golgi markers (as shown here and by others). Lavieu et al. (40) have proposed that the ER and Golgi apparatus in insects, which unlike in mammalian cells is not centralized but spread throughout the cytoplasm, is less efficient for secretion of bulky cargo than mammalian cells that can accommodate and transport it more efficiently through the Golgi ribbon. This difference could explain why *tango1* knockout mice seem to have only collagen secretion defects and die only as neonates (41). However, a complete blockage of the ER might also be prevented by the activity of other MIA3/cTAGE5 family homologs (42–44). In mammalian cell culture experiments, even if loss of *tango1* affects secretion of HRP, the secretion of other overexpressed molecules like alkaline phosphatase is not affected. This could also be because of the presence of other MIA3/cTAGE5 family homologs. By contrast, because there are no other MIA3/cTAGE5 family proteins in *Drosophila*, loss of *tango1* may lead to the accumulation of a wider range of overexpressed proteins and more overt mutant phenotypes than in mammals.

Materials and Methods

Detailed materials and methods are shown in *SI Appendix*.

ACKNOWLEDGMENTS. We thank S. Kraus for technical assistance; N. Jayanandanan for guidance in the early part of this work; S. De Renzis, P. Domingos, D. Gilmour, V. Malhotra, K. Roeper, and members of the M.L. laboratory for helpful discussions; the Vienna Drosophila Resource Center, the Bloomington Drosophila Stock Center, the National Institute of Genetics Fly Stock Center, the Kyoto Drosophila Genetic Resource Center, the Drosophila Genomics Resource Center, and our colleagues M. Affolter, P. Domingos, S. Horne-Badovinac, C. Klämbt, E. Knust, S. Luschnig, C. Rabouille, C. Samakovlis, F. Schnorrer, G. Tanentzapf, and B. Thompson for stocks and reagents; the European Molecular Biology Laboratory (EMBL) Advanced Light Microscopy Facility (ALMF) for continuous support; Zeiss for the support of the ALMF; and P. Bun for his support on image analysis pipelines. FlyBase was used throughout this work and is greatly appreciated. The work was supported through funding from European Molecular Biology Organization, EMBL, Deutsche Forschungsgemeinschaft Grant LE 546/7-1 and the North Rhine-Westphalia Graduate School for Genetics and Functional Genomics. L.D.R.-B. was funded by the EMBL Interdisciplinary Postdoctoral Programme under Marie Curie Actions.

1. Santos AJ, Nogueira C, Ortega-Bellido M, Malhotra V (2016) TANGO1 and Mia2/cTAGE5 (TALI) cooperate to export bulky pre-chylomicrons/VLDLs from the endoplasmic reticulum. *J Cell Biol* 213:343–354.
2. Pfeffer SR (2016) Lipoprotein secretion: It takes two to TANGO. *J Cell Biol* 213: 297–299.
3. Saito K, et al. (2009) TANGO1 facilitates cargo loading at endoplasmic reticulum exit sites. *Cell* 136:891–902.
4. Santos AJ, Raote I, Scarpa M, Brouwers N, Malhotra V (2015) TANGO1 recruits ERGIC membranes to the endoplasmic reticulum for procollagen export. *Elife* 4:e10982.
5. Maeda M, Katada T, Saito K (2017) TANGO1 recruits Sec16 to coordinately organize ER exit sites for efficient secretion. *J Cell Biol* 216:1731–1743.
6. Maeda M, Saito K, Katada T (2016) Distinct isoform-specific complexes of TANGO1 cooperatively facilitate collagen secretion from the endoplasmic reticulum. *Mol Biol Cell* 27:2688–2696.
7. Nogueira C, et al. (2014) SLY1 and Syntaxin 18 specify a distinct pathway for procollagen VII export from the endoplasmic reticulum. *Elife* 3:e02784.
8. Pastor-Pareja JC, Xu T (2011) Shaping cells and organs in Drosophila by opposing roles of fat body-secreted Collagen IV and perlecan. *Dev Cell* 21:245–256.
9. Lerner DW, et al. (2013) A Rab10-dependent mechanism for polarized basement membrane secretion during organ morphogenesis. *Dev Cell* 24:159–168.
10. Liu M, et al. (2017) Tango1 spatially organizes ER exit sites to control ER export. *J Cell Biol* 216:1035–1049.
11. Bard F, et al. (2006) Functional genomics reveals genes involved in protein secretion and Golgi organization. *Nature* 439:604–607.
12. Baer MM, Bilstein A, Leptin M (2007) A clonal genetic screen for mutants causing defects in larval tracheal morphogenesis in Drosophila. *Genetics* 176:2279–2291.
13. Tsarouhas V, et al. (2007) Sequential pulses of apical epithelial secretion and endocytosis drive airway maturation in Drosophila. *Dev Cell* 13:214–225.
14. Raote I, et al. (2017) TANGO1 assembles into rings around COPII coats at ER exit sites. *J Cell Biol* 216:901–909.
15. Misra S, et al. (2002) Annotation of the Drosophila melanogaster euchromatic genome: A systematic review. *Genome Biol* 3:research0083.1–research0083.22.
16. Wilkin MB, et al. (2000) Drosophila dumpy is a gigantic extracellular protein required to maintain tension at epidermal-cuticle attachment sites. *Curr Biol* 10:559–567.
17. Öztürk-Çolak A, Moussian B, Araújo SJ (2016) Drosophila chitinous aECM and its cellular interactions during tracheal development. *Dev Dyn* 245:259–267.
18. Ray RP, et al. (2015) Patterned anchorage to the apical extracellular matrix defines tissue shape in the developing appendages of Drosophila. *Dev Cell* 34:310–322.
19. Schottenfeld-Roames J, Rosa JB, Ghabrial AS (2014) Seamless tube shape is constrained by endocytosis-dependent regulation of active Moesin. *Curr Biol* 24: 1756–1764.
20. Petley-Ragan LM, Ardiel EL, Rankin CH, Auld VJ (2016) Accumulation of laminin monomers in Drosophila glia leads to glial endoplasmic reticulum stress and disrupted larval locomotion. *J Neurosci* 36:1151–1164.
21. Tiwari P, Kumar A, Das RN, Malhotra V, VijayRaghavan K (2015) A tendon cell specific RNAi screen reveals novel candidates essential for muscle tendon interaction. *PLoS One* 10:e0140976.
22. Knowles-Barley S, Longair M, Armstrong JD (2010) BrainTrap: A database of 3D protein expression patterns in the Drosophila brain. *Database (Oxford)* 2010:baq005.
23. Hamill KJ, Kligys K, Hopkinson SB, Jones JC (2009) Laminin deposition in the extracellular matrix: A complex picture emerges. *J Cell Sci* 122:4409–4417.
24. Coelho DS, et al. (2013) Xbp1-independent Ire1 signaling is required for photoreceptor differentiation and rhabdomere morphogenesis in Drosophila. *Cell Rep* 5: 791–801.
25. Ryoo HD, Domingos PM, Kang MJ, Steller H (2007) Unfolded protein response in a Drosophila model for retinal degeneration. *EMBO J* 26:242–252.
26. Riedel F, Gillingham AK, Rosa-Ferreira C, Galindo A, Munro S (2016) An antibody toolkit for the study of membrane traffic in Drosophila melanogaster. *Biol Open* 5: 987–992.
27. Zhai B, Villén J, Beausoleil SA, Mintseris J, Gygi SP (2008) Phosphoproteome analysis of Drosophila melanogaster embryos. *J Proteome Res* 7:1675–1682.
28. Hollien J, Weissman JS (2006) Decay of endoplasmic reticulum-localized mRNAs during the unfolded protein response. *Science* 313:104–107.
29. Baer MM, Palm W, Eaton S, Leptin M, Affolter M (2012) Microsomal triacylglycerol transfer protein (MTP) is required to expand tracheal lumen in Drosophila in a cell-autonomous manner. *J Cell Sci* 125:6038–6048.
30. Ishikawa Y, Ito S, Nagata K, Sakai LY, Bächinger HP (2016) Intracellular mechanisms of molecular recognition and sorting for transport of large extracellular matrix molecules. *Proc Natl Acad Sci USA* 113:E6036–E6044.
31. Martinek N, Shahab J, Saathoff M, Ringuette M (2008) Haemocyte-derived SPARC is required for collagen-IV-dependent stability of basal laminae in Drosophila embryos. *J Cell Sci* 121:1671–1680.
32. Kivirikko KI, Myllyharju J (1998) Prolyl 4-hydroxylases and their protein disulfide isomerase subunit. *Matrix Biol* 16:357–368.
33. Schotman H, Karhinen L, Rabouille C (2008) dGRASP-mediated noncanonical integrin secretion is required for Drosophila epithelial remodeling. *Dev Cell* 14:171–182.
34. Norum M, et al. (2010) Trafficking through COPII stabilises cell polarity and drives secretion during Drosophila epidermal differentiation. *PLoS One* 5:e10802.
35. Shahab J, et al. (2015) Loss of SPARC dysregulates basal lamina assembly to disrupt larval fat body homeostasis in Drosophila melanogaster. *Dev Dyn* 244:540–552.
36. Kramer J (2005) Basement membranes. *WormBook*, 10.1895/wormbook.1.138.1.
37. Call ME, Wucherpfennig KW (2004) Molecular mechanisms for the assembly of the T cell receptor-CD3 complex. *Mol Immunol* 40:1295–1305.
38. Zhang YC, Zhou Y, Yang CZ, Xiong DS (2009) A review of ERGIC-53: Its structure, functions, regulation and relations with diseases. *Histol Histopathol* 24:1193–1204.
39. Zacharogianni M, Aguilera-Gomez A, Veenendaal T, Smout J, Rabouille C (2014) A stress assembly that confers cell viability by preserving ERES components during amino-acid starvation. *Elife* 3:e04132.
40. Lavieu G, et al. (2014) The Golgi ribbon structure facilitates anterograde transport of large cargoes. *Mol Biol Cell* 25:3028–3036.
41. Wilson DG, et al. (2011) Global defects in collagen secretion in a Mia3/TANGO1 knockout mouse. *J Cell Biol* 193:935–951.
42. Saito K, et al. (2011) cTAGE5 mediates collagen secretion through interaction with TANGO1 at endoplasmic reticulum exit sites. *Mol Biol Cell* 22:2301–2308.
43. Tanabe T, Maeda M, Saito K, Katada T (2016) Dual function of cTAGE5 in collagen export from the endoplasmic reticulum. *Mol Biol Cell* 27:2008–2013.
44. Saito K, et al. (2014) Concentration of Sec12 at ER exit sites via interaction with cTAGE5 is required for collagen export. *J Cell Biol* 206:751–762.